Title: Glutamate NMDA receptors containing GluN2C subunit relay the reward signal of the ventral tegmental area upon dorsal raphe stimulation

Running tittle: VTA NMDA GluN2C subunit relays the reward signal

Authors : Hernandez, Giovanni [1]; Poirier Emmanuelle[1]; Lebied Karim[1], Kouwenhoven, Willemieke M[2]; Lévesque, Daniel[3]; Rompré, Pierre-Paul[1]

(1) Département de neurosciences (Faculté de médecine), (2) Département de pharmacologie et physiologie (Faculté de médecine), (3) Faculté de Pharmacie, Université de Montréal, Montréal, QC.

Corresponding Author(s): Hernandez, Giovanni. Mailing address: Neuroscience Department Douglas Research Hospital, 6875 Boulevard LaSalle. E-2107, Perry Pavilion.Montréal, QC H4H 1R3. E-mail : giovanni.hernandez.comtl@ssss.gouv.qc.ca. Phone number 514-8308293

Rompré, Pierre-Paul. Mailing address Département de Neurosciences Université de Montréal Pavillon Paul-G. Desmarais, 2960 Chemin de la Tour. Montréal, QC H3T 1N8.e-mail : pierre-paul.rompre@umontreal.ca Phone number : 514-3436111 ext 35351

Key words: NMDA receptors, GluN2C, Dorsal Raphe, Dopamine, Glutamate, Reward.

Abstract:

Background: Glutamate relays the reward signal from the dorsal raphe (DR) to ventral tegmental area (VTA) dopamine (DA) neurons. However, its role is complex and not clearly understood. We measured NMDA receptors subunits expression in limbic brain areas and studied the effects of VTA down-regulation of GluN2C subunit-containing NMDA receptor on the reward signal that arises from DR electrical stimulation.

Methods: Via qPCR, we identified the relative composition of the different GluN2 NMDA receptors subunits in several brain areas. Then we used fluorescent *in situ* hybridization (FISH) to evaluate the colocalization of Grin2c and Tyrosine hydroxylase (Th) mRNA in VTA neurons. To assess the role of GluN2C in reward pursuit; we downregulated this receptor using small interfering RNA (siRNA) in rats self-stimulating for electrical pulses delivered to the DR. To delineate further the specific role of GluN2C in relaying the reward signal, we pharmacologically altered the function of VTA NMDA receptors by either bilaterally microinjecting the NMDA receptor antagonist PPPA or the glutamate transporter inhibitor (GLT-1), Dhk.

Results: We identified that GluN2C is the most abundant NMDA receptor subunit expressed in the VTA. FISH revealed that a substantial number of TH+ neurons colocalize with Grin2C. The siRNA manipulation produced a selective down-regulation of GluN2C and a significant reduction in reward pursuit. Interestingly, PPPA and DHK respectively enhanced and suppressed reward pursuit, but only in rats that received the non-active RNA sequence.

Conclusion: The present results suggest that VTA Glutamate neurotransmission relays the reward signal initiated by DR stimulation by acting on GluN2C NMDA receptors.

Introduction

The dorsal raphe (DR) nucleus contains a heterogeneous group of neurons that send one of the highest density of projections to the ventral tegmental area (VTA) (Watabe-Uchida, Zhu, Ogawa, Vamanrao, & Uchida, 2012), the origin of dopamine (DA) pathways which are implicated in reward and motivation (G. Hernandez, Trujillo-Pisanty, Cossette, Conover, & Shizgal, 2012; Giovanni Hernandez, Breton, Conover, & Shizgal, 2010; Salamone, 1991; Schultz, 1997; R a Wise & Rompre, 1989; Roy a Wise, 2004). Previous studies showed that DR electrical stimulation triggers a strong reward signal (Rompre & Miliaressis, 1985; Simon, Le Moal, & Cardo, 1976) that propagates to the VTA where it activates DA-like neurons (Boye & Rompré, 1996; Moisan & Rompre, 1998). The DR contains a large number of serotoninergic neurons (Jacobs & Azmitia, 1992), but it also contains glutamatergic, nitric oxide synthase, GABAergic and dopaminergic neurons (Vasudeva, Lin, Simpson, & Waterhouse, 2011). Paired-pulse stimulation experiments showed that the refractory periods of the reward-relevant axons that linked DR to VTA are incompatible with those of serotoninergic neurons (Boye & Rompré, 1996; Rompré & Miliaressis, 1987; Wang & Aghajani, 1977), suggesting that the reward signal is carried to the VTA by non-serotonergic projections. Indeed, studies with optical stimulation showed that selective activation of DR glutamatergic neurons and their VTA terminals is rewarding (Liu et al., 2014; Mcdevitt et al., 2014; Qi et al., 2014). These terminals established asymmetrical synapses with DA neurons (Qi et al., 2014; Sesack, Carr, Omelchenko, & Pinto, 2003), and VTA glutamate release stimulates DA activity leading to enhancement of extracellular DA in the nucleus accumbens, a limbic region that plays a key role in reward and motivation(Qi et al., 2014). According to Qi et al.'s (2014) data, AMPA receptors mediated the transmission of the DR reward signal to VTA mesoaccumbens DA neurons. Several characteristics of the interaction between glutamate and DA, however, also suggest a role for glutamate NMDA receptors (NMDAR).

Glutamate inputs to VTA DA neurons make them switch from a tonic, single-spike irregular firing pattern, to a phasic burst firing pattern(Chergui et al., 1993a; Grace & Bunney, 1984; Hyland, Reynolds, Hay, Perk, & Miller, 2002) associated with enhanced accumbens DA release (Suaud-Chagny, Chergui, Chouvet, & Gonon, 1992; Tsai et al., 2009). Activation of NMDARs mediates the transition from tonic to phasic burst firing (Chergui et al., 1993b; Johnson, Seutin, & North, 1992; P. G. Overton & Clark, 1997; Parker et al., 2010; Zweifel et al., 2009), and DA burst firing conveys motivationally relevant signals to anterior forebrain regions that control executive functions (P. G. Overton & Clark, 1997) and encode reward prediction errors; as such it is associated with the acquisition of appetitive and aversive tasks (Zweifel et al., 2009).

Interestingly, the identity of the NMDAR responsible for relaying DR reward signal to VTA DA neurons is not known. NMDARs are heteromeric or triheteromeric complexes composed of two obligatory GluN1 subunits that cluster with GluN2 and/or GluN3 subunits (McIlhinney et al., 1998; Pérez-Otaño et al., 2001). In a previous study from our group, we reported that a downregulation of GluN1 in the VTA neurons, which produces a non-selective reduction in NMDAR, results in a selective attenuation of reward induced by DR electrical stimulation (Giovanni Hernandez, Khodami-Pour, Lévesque, & Rompré, 2015). But, we could not identify the GluN1 subunit partner because a similar downregulation of GluN2A or GluN2D subunit failed to alter reward pursuit (Giovanni Hernandez et al., 2015). Also, selective pharmacological blockade of VTA GluN2B subunits had no effect on the reward signal arising from the DR (Bergeron & Rompré, 2013). Here, we report that the mRNA for GluN2C is expressed in the VTA in higher concentration than mRNA for the other subunits (A, B, or D) and co-localizes within tyrosine hydroxylase positive (Th+) neurons, and that NMDAR containing GluN2C subunits are responsible for conveying the DR rewarding signal to VTA neurons.

Materials and Methods

Subjects and surgery

Twenty-two (22) male Long-Evans rats (Charles River, St-Constant, QC) weighing between 350-400 g at the time of the surgery were used. Rats were individually housed in a temperature- and humidity- controlled room with a 12-h light-dark cycle (lights on at 06:00 h) and *ad libitum* access to food and water. After a minimum 7-day period of acclimation to the housing, environment rats were anesthetized with isoflurane (2.5-3.5% O2, 0.6 L/min) and stereotaxically implanted according to Paxinos and Watson (2007) coordinates with 26-gauge guided canulae (HRS Scientific, Montreal, Canada) aimed bilaterally at the VTA (-5.5 AP, 3.2 ML at an 18° angle, 6.5 DV from the skull surface) and a stainless steel monopolar electrode aimed at the DR (-7.6 AP, 0 ML, 6.6 DV from the skull surface). Detailed surgical procedures can be found in Bergeron and Rompré (2013). All procedures were approved by the Animal Care and Use Committee of the Université de Montréal in accordance with the guidelines of the Canadian Council on Animal Care.

siRNAs and Drugs

Downregulation of selective NMDAR subunit expression was achieved using a pre-validated small interfering RNA (siRNA) sequence against rat glutamate ionotropic receptor NMDA type subunit 2C (Grin2c) mRNA, which encodes the GluN2C protein subunit (Silencer™ select pre-designed siRNA # 4390771, siRNA ID s127815, ThermoFisher Scientific) and a non-active RNA sequence (Silencer™ select negative control #4390844, ThermoFisher Scientific). The deprotected, duplexed, desalted siRNA was mixed with a cationic lipid transfection carrier N-[1-(2,3-Dioleoyloxy)propyl]-N, N, N-trimethyl-ammonium methylsulfate (DOTAP) (Roche Applied Sciences, Indianapolis, IN), which showed high efficacy for *in vivo* transfection (Salahpour, Medvedev, Beaulieu, Gainetdinov, & Caron, 2007). The final solution contained 10 µg of the active or inactive siRNA and 1 µg of DOTAP per µl.

PPPA (2R,4S)-4-(3-Phosphopropyl)-2-piperidinecarboxylic acid, a competitive GluN2A-preferred NMDAR antagonist (Tocris, Ellisville, MI, USA), and Dihydrokainate (Dhk), a selective inhibitor for the glial GLT-1 transporter (Tocris, Ellisville, MI, USA), were dissolved in sterile 0.9% saline and stored frozen in 40–50 µl aliquots. Drug solutions were thawed just before testing and used only once. PPPA was injected into the VTA at a dose of 0.825 nmol/0.5µl/side, as previously described (reference), and Dhk was injected into the VTA at a dose of 5 nmol/0.5µl/side. Drug doses are expressed as salts.

Self-stimulation training

Each of the rats was shaped to lever press for a 0.4-sec train of cathodal, rectangular, constant-current pulses, 0.1 msec in duration, delivered at a frequency of 98 Hz. For a detailed shaping procedure, see (Bergeron & Rompré, 2013). Once the rat nose-poked consistently for currents between 125 and 400 µA, a rate vs. pulse-frequency curve was obtained by varying the stimulation frequency across trials over a range that drove the number of rewards earned from maximal to minimal levels; the stimulation frequency was decreased from trial to trial by approximately 0.05 log10. Each trial for obtaining the rate-frequency sweep lasted for 55-s followed by a 15-s inter-trial interval during which stimulation was not available. The beginning of each trial was signaled by 5 trains of non-contingent priming stimulation delivered at a rate of 1 per second. Four sweeps were run daily, and the first sweep was considered a warm-up and discarded from the analysis. The data relating the rate-frequency was fitted to a sigmoid described by the following equation y=Min+((Max-Min))/(1+[10]^((x50-x)*p)) where Min is the lower asymptote, Max is the upper asymptote, x50 is the position parameter denoting the frequency at which the slope of the curve is maximal, and p determines the steepness of the sigmoid curve. The resulting fit was used to derive an index of reward defined as the pulse-frequency sustaining a half-maximal rate of responding (M50). Self-stimulation behavior was considered stable when the M50 values varied less than 0.1 log unit for three consecutive days.

Prior to the siRNA injections or drug administration, sterile 0.9% saline was microinjected into the VTA to habituate the animals to the injection procedure. Bilateral injections were made by inserting an injection cannula (Model C315I HRS Scientific, Montreal, Canada) that extended 2 mm beyond the guide cannula tip. The injection cannula was connected to a 5 µl Hamilton microsyringe via polyethylene tubing. A total volume of 0.5 µl was injected in each hemisphere simultaneously over a 60-s period. The rate of delivery was controlled by an infusion pump (Harvard Instruments, Holliston, MA). The injection cannulae were left in place for an additional 60-s to allow diffusion into the tissue. After the microinjection, the subjects were put into the operant boxes and allowed to self-stimulate. Results from this test were not included in the analysis. Baseline data were collected one week after this first saline microinjection. Once a stable baseline was obtained, pre-validated siRNA (5 µg per side) against GluN2C or the non-active RNA sequence was injected bilaterally into the VTA for two consecutive days. Reward thresholds were measured 24-h after each injection. After 24 h the last threshold determination rats received either a bilateral VTA microinjection of the NMDA antagonist, PPPA, or the glutamate transporter inhibitor (GLT-1), Dhk, and reward thresholds were measured again immediately after the injection for 120 min (see supplementary Fig. S1 for experiment timeline).

Western Blot

Rats were decapitated immediately after the last behavioral test. Brains were removed and directly placed on an ice-cold brain matrix and sectioned coronally. The VTA was dissected out on an ice-cooled plate from a 0.75-1-mm slice using a 15-gauge tissue punch. The tissue was put in a 1 ml Eppendorf and then immediately frozen at -80°C until biochemical experiments were performed. VTA samples were mechanically homogenized in lysis buffer [10 mM Tris–HCl (pH 6.8), 2% SDS, and a cocktail protease inhibitor (Roche)]. The protein concentrations of the tissue samples were measured using the BCA ™ protein assay kit (Pierce, USA). Equal amounts of protein (10 µg) were dissolved into 25 µl lysis buffer (which contained 4.5 µl 5X loading buffer and 0.5 µl β-mercaptoethanol), boiled at 95°C for 5 min,

and then subjected to SDS polyacrylamide gel electrophoresis (PAGE) with 8% polyacrylamide and transferred to polyvinylidene difluoride (PVDF) membrane (BioRad Laboratories). The membranes were blocked for 1 h in Tris-Buffered Saline with Tween 20 (TBST) buffer with 5% bovine serum albumin (BSA) and were incubated with primary rabbit anti-β-actin antibody (Millipore Sigma, cat. #SAB5600204) at 1:20000, with either primary mouse anti-GluN2C antibody (Novus Biological, cat. no. #NBP2-29809) or mouse anti-GluN2A antibody (Millipore, cat. #SAB5200897) at 1:500 overnight at 4°C. After rinsing 4 times with TBST for 5 min, the membranes were incubated with Horse Raddish Peroxidase (HRP)-conjugated goat anti-mouse IgG secondary antibody (Cell Signaling, cat. #7076) at 1:20000 (to detect GluN2C or GluN2A) or HRP-conjugated goat anti-rabbit IgG secondary antibody (Cell Signaling, cat. #7074) at 1:40000 (to detect β-actin) for 1 h. The membrane protein bands were detected with ECL (BioRad) and visualized on the Chemidoc Biorad system (BioRad). The band densities were measured and analyzed with Image Lab software (BioRad), and protein levels were normalized over β-actin. The different subunits of the NMDAR were expressed as a percentage of control.

Double Fluorescent *In Situ* Hybridization (FISH)

Naive Long-Evans male rats were anesthetized using an overdose of intraperitoneal ketamine 50 mg/kg, xylazine 5 mg/kg, and acepromazine 1 mg/kg perfused intracardially with ice-cold PBS. After removal, brains were rapidly frozen in dry ice-cooled 2-methyl butane (Fisher Scientific, Hampton, NH, USA). Coronal sections of the VTA at 10 µm were obtained using a cryostat and mounted onto superfrost slides (Fisher Scientific Ltd, Nepean, ON, Canada). Coronal cryosections were prepared, air-dried, fixed in 4% paraformaldehyde, and acetylated in 0.25% acetic anhydride/100 mM triethanolamine (pH 8) followed by incubation for 30 minutes at room temperature in hybe-solution. Then, slices were incubated overnight at 60°C in 100 µl of hybe-solution buffer containing 20 ng digoxigenin (Dig)-labeled probes (see below) for colorimetric detection (Roche, cat. #11277073910) or 20 µg of fluorescein-

labeled probes (see below) for fluorescent detection (Roche, cat. #11685619910). After hybridization, sections were washed at 60°C with SSC buffers of decreasing strength (5X-0.2X), then washed at room temperature with 0.2X SSC and maleic acid buffer containing tween 20 (MABT). After washing, sections were blocked for 30 minutes with 20% FBS and 1% blocking solution. For colorimetric detection, Dig epitopes were detected with alkaline phosphatase-coupled anti-Dig fab fragments antibody at 1:2500 (Millipore Sigma, cat. #11093274910) and signal revealed with Nitro Blue Tetrazolium chloride/5-Bromo-4-Chloro-3-Indolyl Phosphate, toluidine salt (NBT/BCIP) alkaline phosphatase chromogen substrate solution (SigmaAldrich).

For fluorescent detection, sections were incubated with HRP-conjugated anti-fluorescein antibody at 1:500 concentration. Signals were revealed with the Tyramide Signal Amplification (TSA plus biotin) kit (PerkinElmer, cat. #NEL749A001KT) at 1:100 concentration followed by incubation with neutravidin Oregon Green conjugated at 1:500 (Invitrogen, cat. #A-6374). HRP-activity was stopped by incubation of sections in 0.1 M glycine and 3% H_2O_2. Dig epitopes were detected with HRP-conjugated anti-Dig antibody at 1:1000 (Roche cat. #11207733910) and revealed with the TSA kit (PerkinElmer, cat. #NEL704A001KT) using Cy3 tyramide at 1:100. All sections were counterstained using DAPI and mounted using Fluoromount (ThermoFisher Scientific, cat. #00-4958-02).

Double FISH was performed with RNA probes labeled with digoxigenin (Dig) for tyrosine hydroxylase and RNA probe labeled with Fluorescein for Grin2c, consisting of a 678 bp fragment, (Fw primer: 5'-ctactgctcccgtgaagagg-3', Rv primer: 5'-agagcttggtgtaggggtt-3'). The tyrosine hydroxylase probe consisting of fragment of 1142 bp was a kind gift from Prof. Marten Smidt (University of Amsterdam). Cells were automatically counted using ImageJ FIJI software (NIH, USA).

qRT-PCR analysis

Because no study has been carried out to determine the extent of the different NMDAR subunits in the VTA, or in other limbic brain regions involved in reward and motivation, we carried the following real-time quantitative RT-PCR study. Brain punches from the prefrontal cortex (PFC), nucleus accumbens (Nac), lateral hypothalamus (LH), habenula (Hab), amygdala (Amyg), bed nucleus of the stria terminalis (BNst), ventral pallidum (VP), hippocampus (Hipp), pedunculopontine tegmental nucleus (PPtg), ventral tegmental area (VTA), rostromedial tegmental nucleus (RMtg) and raphe nucleus of four (n=4) naive Long-Evans male rats were taken. Total RNA was extracted using trizol and purified on mini spin columns (RNeasy Kit protocol, Qiagen, Toronto, ON, Canada). All RNA samples were determined to have 260/280 and 260/230 values >1.8, using the Nanodrop 1000 system (Thermo Scientific, Toronto, ON, Canada). We assessed RNA integrity by the presence of well-defined 28S and 18S ribosomal bands and RNA integrity number ≥8, using 2100 bioanalyzer (Agilent). Reverse transcription (RT) for Grin2a, Grin2b, Grin2c, Grin2d, glyceraldehyde-3-phosphatedehydrogenase (Gapdh) and hypoxanthine phosphoribosyltransferase (Hprt) were performed (see primer sequences in supplementary Table 1). Real-time PCR, using TaqMan assay was carried out with an Applied Biosystems 7900HT RT PCR system at the Institute for Research on Immunology and Cancer (IRIC) genomic platform (https://genomique.iric.ca/). Data were analyzed using the relative quantification method ($\Delta\Delta$ ct), and the levels of transcripts were normalized with both the expression of the reference (housekeeping) genes, Gapdh and Hprt.

Data Analysis

The fit of the rate frequency data and M50 value were obtained using Matlab (Natick, MA). Differences in M50 values and protein levels were assessed using t-test. Data analysis was performed using Statistica v12 (Tulsa, OK), and graphics were done in Origin v9 (Northamptom, MA).C

Results

Expression of NMDAR subunit mRNAs (Grin2a-d) in the VTA and other limbic areas

In order to understand how glutamate signals are being relayed through the limbic and DA system, we first investigated the distribution of different NMDAR subunits throughout these regions. We performed qPCR on mRNA taken from all relevant regions (Fig. 1: the prefrontal cortex (PFC), nucleus accumbens (Nac), lateral hypothalamus (LH), habenula (Hab), amygdala (Amyg), bed nucleus of the stria terminalis (BNST), ventral pallidum (VP), hippocampus (Hipp), pedunculopontine tegmental nucleus (PPtg), ventral tegmental area (VTA), rostromedial tegmental nucleus (RMtg) and raphe nucleus). As expected, mRNA concentrations vary notably across brain areas, although in all examined brain regions, we observed that the expression of Grin2d subunit remained relatively low compared to other subunits. In the hippocampus, the mRNA for the Grin2a and Grin2b subunits are the most abundant, followed by Grin2c. In the prefrontal cortex, the Grin2b mRNA is the most abundant, followed by Grin2a and Grin2c. Similar relative distribution of mRNA for the different NMDA subunits can be seen in the amygdala, habenula, and the bed nucleus of the stria terminalis. For the nucleus accumbens and the ventral pallidum, Grin2b mRNA is the most abundant, followed by Grin2c and Grin2a. The lateral hypothalamus contains a similar concentration of mRNA for the Grin2a and Grin2b subunit. Interestingly, in mesencephalic regions, namely the pedunculopontine tegmental nucleus, the VTA, the rostromedial tegmental nucleus, and the DR, the Grin2c mRNA is the most abundant.

To confirm and elaborate on the observation that VTA neurons express significant levels of Grin2c, we performed an independent set of experiments to investigate the spatial expression of Grin2c in the mesencephalon. The Allen Brain Atlas displays the expression of Grin2c in the mesencephalon, with expression in the red nucleus (arrowhead, Fig 2A) and SN and VTA region (arrow, Fig 2A) (Allen Institute for Brain Science, 2010; Lein et al., 2007). Using the same probe, we confirmed the ample expression of Grin2c in the midbrain (Fig 2A). To verify if Grin2c is expressed in DA neurons, we

performed double-labeling fluorescent *in situ* hybridization and observed co-expression of Th transcript and Grin2c in the VTA (Fig 2B). Quantitative analysis shows that the level of colocalization of Grin2c and TH in DA neurons is around 46% (S.E.M.= 7.83) (Fig. 2C and supplementary Fig. S2). Together, these data suggest that Grin2c might be a relevant component in transmitting the glutamatergic signals by DA VTA neurons.

Validation of siRNA effects on NMDA receptor subunit protein levels

Knowing that the Grin2c is significantly expressed in DA VTA neurons, we set out to determine its involvement in relaying the glutamate reward signal. To do so, we designed a strategy to specifically down-regulate NMDA receptor GluN2C *in vivo*: we injected adult rats bi-laterally with siRNA against Grin2c or a scrambled siRNA as a control in the VTA (-5.5 AP, 3.2 ML at an 18° angle, 6.5 DV from the skull surface). To confirm both the efficacy and the specificity of the Grin2c siRNA, we performed western blot for GluN2C and GluN2A on total homogenates of VTA (Immediately after the last behavioral test). Microinjections of siRNA against Grin2c produced a significant 41% (S.E.M.= 3.22) decrease in the expression of NMDAR GluN2C receptor when compared against scrambled control [$t_{(10)}$=2.43; $p<0.05$](Fig. 3A). Moreover,The active siRNA was selective for GluN2C since we observed no change in protein expression of the GluN2A subunit [$t_{(10)}$=0.28; $p>0.05$] (Fig. 3B).

Downregulation of the GluN2C subunit in VTA strongly reduces Dorsal Raphe reward signal

The selective downregulation of the GluN2C NMDA subunit produced a decrease in reward-seeking behavior. Figure 4 shows the behavioral data collected 24 h after the last siRNA microinjection for representative subjects. Intra-VTA microinjections of the active siRNA against Grin2c produced a rightward displacement of the curve that relates the nose-poke rate to the pulse frequency (R/F curve; Fig. 4C and 4C'), reflecting a reduction in transmission of the reward signal within the VTA. In contrast,

VTA microinjections of the inactive RNA sequence did not affect the transmission of the reward signal as it produced no significant displacement of the R/F curve (Fig. 4A and 4A').

To further delineate the specific role of GluN2C in relaying the reward signal in VTA neurons, we used a pharmacological approach the target NMDAR's in animals that had received either a scrambled or Grin2c siRNA injection. First, in the animals microinjected with the inactive siRNA, the NMDA antagonist, PPPA, enhanced the reward signal in the VTA; it produced a leftward displacement of the R/F curve (Fig. 4B) so that lower frequencies delivery to the DR were required to generate reward. Second, the glutamate transporter blocker, Dhk, produced the opposite effect, it attenuated the reward signal in the VTA and the R/F curve is thus shifted to the right (Fig. 4B'). Interestingly, PPPA and Dhk failed to alter the reward signal (no displacement of the R/F curve) in the animals microinjected with the active Grin2c siRNA (Fig. 4D and 4D').

Figure 5 shows the average changes in the M50 reward index (Fig. 5A) and in maximal response (Fig. 5B). Intra-VTA injection of siRNA against Grin2c produced a 53.2% (SEM = 10.97) increase in M50 when compared against their baseline, whereas the M50 of the rats that received the non-active RNA only changed 1.2 % (S.E.M.= 2.22). The increase in M50 observed in the subjects that received the siRNA against Grin2c is significantly different from that of the ones that received the scramble sequence [$t_{(20)}$=2.79 $p<0.05$] and reflect a significant reduction in transmission of DR reward signal to VTA neurons. The active siRNA also produced a small but significant 17.3% (S.E.M.=3.12) decrease in the maximum response rate (Fig. 5B) [$t_{(20)}$= 2.16; $p<0.05$].

The pharmacological manipulation of VTA glutamate using PPPA and Dhk produced reliable changes in M50 and maximum response rate only in the animals that received the inactive siRNA treatment. PPPA enhanced the reward signal (reduction in M50 index, Fig. 6A). M50 decreased in average 18.7 % (S.E.M. = 2.38) and maximum response rate increased in average 25% (S.E.M. = 4.15; Fig.

6B). As seen before, Dhk produced the opposite effect, attenuating the reward signal in the VTA (increase in M50; Fig. 6C). M50 increased in average 18.9 % (S.E.M. = 7.24), and maximum response rate decreased in average 25.7 % (S.E.M. = 4.15, Fig. 6D). For the subjects that received the siRNA against Grin2c, PPPA increased the M50 by 2% (SEM = 4.17) and the maximum response rate by 3.6% (S.E.M=4.4) (Fig. 6A and 6B). Dhk also produced minimal effects; it increased the M50 by 2% and decreased the maximum rate by 3.9% (S.E.M=2.8) (Fig. 6C and 6D). The differences between the inactive and active siRNA are significant for the changes produced in M50 for both PPPA [$t_{(9)}$=4.62 $p<0.05$] and Dhk [$t_{(10)}$=4.10; $p<0.05$] as well as for the changes produced in the maximum rate for PPPA [$t_{(9)}$=3.05; $p<0.05$] and Dhk [$t_{(10)}$=4.11; $p<0.05$]]. Together these data suggest the GluN2C subunit is vitally important to relay the reward signal in VTA neurons.

Discussion

Glutamate containing terminals establish synaptic contacts with DA neurons (Carr & Sesack, 2000; Omelchenko & Sesack, 2009) and rewarding electrical stimulation is associated with an increase in VTA glutamate release (You, Chen, & Wise, 2001). Some of those VTA terminals come from the DR, which sends the highest number and density of glutamatergic projections (Watabe-Uchida et al., 2012). NMDA receptors mediate glutamate activation of DA neurons. Iontophoretic administration of NMDA receptor antagonists (P. Overton & Clark, 1992), as well as genetic deletion of NMDA receptor GluN1 subunit from DA neurons, selectively attenuate DA phasic firing and reduces learning in cue-dependent learning tasks (Zweifel et al., 2009). VTA downregulation of the GluN1 subunit also produces a decrease in reward pursuit (Giovanni Hernandez et al., 2015). That the deletion or downregulation of the GluN1 subunit produces profound effects is not surprising, as this subunit is a necessary component in the formation of functional NMDA receptor heteromeric complexes (Monyer et al., 1992; Nakanishi, 1992).

Here we isolated the specific NMDA receptor subunit responsible for the relay of the reward signal initiated by DR stimulation to VTA neurons. We demonstrated that the NMDA receptor GluN2C subunit, in the VTA, is a necessary component for the transmission of the rewarding signal arising from the DR. Our selective GluN2C subunit downregulation *via* siRNA produced a significant reduction in reward pursuit, as well as, a change in the performance capacity. These attenuations are inferred by the rightward displacement of the R/F curve and the downward shift of the upper asymptote (Miliaressis, Rompre, Laviolette, Philippe, & Coulombe, 1986). Both effects might be associated with a reduction in the nucleus accumbens DA release since this decrease can affect both reward and motor function (Stellar, Kelley, & Corbett, 1983). Electrical or optical stimulation of DR neurons produces an increase in DA cell firing and DA phasic release (Giovanni Hernandez, Cossette, Shizgal, & Rompré, 2016; Moisan & Rompre, 1998; Qi et al., 2014), via glutamatergic afferents to the VTA (Liu et al., 2014; Mcdevitt et al., 2014; Qi et al., 2014). The substantial reduction in the GluN2C input likely decreases the glutamatergic excitability onto DA neurons, reducing the overall DA release in terminal areas. The reduction of reward pursuit is specific to GluN2C since previous downregulation of GluN2A or/and GluN2D did not produce a significant change in the curve that relates stimulation of the DR with nose-poke behavior (Giovanni Hernandez et al., 2015).

Our double fluorescent hybridization data shows that the GluN2C receptors are colocalized in TH+ cells. This observation is in line with single-cell expression profiling on DA neurons, which shows that the gene Grin2c is expressed in mesocorticolimbic DA neurons (Anderegg, Poulin, & Awatramani, 2015; Poulin, Gaertner, Moreno-Ramos, & Awatramani, 2020; Saunders et al., 2018). Using qPCR, we observed that this subunit is the most abundantly expressed in the DR and VTA when contrasted against the other three Grin2 subunits. In fact, the Grin2c subunit is expressed in all the brain areas observed of the adult rat brain, but its relative expression changes accordingly to where in the anterior-posterior axis, it is measured. While the Grin2a and Grin2b subunits are the most abundant subunits in the

anterior and medial parts of the brain, the balance shifts towards Grin2c in posterior brain areas. This observation is significant because, until recently not many studies have been done regarding the role of this NMDA receptor subunit, which was believed to be confined to the cerebellum, thalamus, and olfactory bulb and to be present at very low levels in the hippocampus of the adult rodent brain (Monyer, Burnashev, Laurie, Sakmann, & Seeburg, 1994; Wenzel et al., 1995). However, present results and recent observations using novel reporter mice (Ravikrishnan et al., 2018) suggest that this is not the case. Moreover, there is accumulating evidence that the NMDA receptor containing the GluN2C subunit plays an important role in several domains. For example, NMDA receptors containing GluN2C are required for the acquisition of conditioned fear and working memory because Grin2c knockout mice show deficits in associating cues with aversive consequences as well as navigating an eight-arm radial maze (Hillman, Gupta, Stairs, Buonanno, & Dravid, 2011). Also, they spend more time immobile in the forced swim test (Shelkar et al., 2019). At the cortical level, this receptor controls the balance of excitatory and inhibitory activity in the medial prefrontal cortex, since Grin2c knockout mice have reduced excitatory postsynaptic currents, increased inhibitory postsynaptic currents and reduced spine density (Gupta et al., 2016).

Our pharmacological manipulation with either PPPA or with the selective blockade of astrocytic glutamate transporter GLT-1, Dhk, only produced reliable changes in M50 and maximum response rate in the animals that received the inactive siRNA. PPPA produced a decrease in M50 and an increase in the maximum response rate. These observations are consistent and replicated previous results (Bergeron & Rompré, 2013; Ducrot, Fortier, Bouchard, & Rompré, 2013; Giovanni Hernandez et al., 2015), whereas Dhk produced the opposite effect. The most likely mechanism by which PPPA alters reward pursuit is by antagonizing an excitatory drive to VTA inhibitory interneurons. These interneurons maintain a strong inhibitory drive over DA neurons, so blocking this inhibition would allow DA neurons to pass from a

silent state into a tonic firing state, increasing the likelihood of DA neurons to fire into phasic mode given a glutamate signal.

On the other hand, the increase in the availability of Glutamate via blockade of the glutamate transporter GLT-1 would increase the overall inhibitory drive onto DA cells, therefore, reducing the total number of DA neurons to be readily excited by glutamatergic inputs. *In vitro* electrophysiological recordings had shown that local inhibitory postsynaptic potentials participate in this feed-forward inhibition and alter DA cell firing (Bonci & Malenka, 1999; Nugent & Kauer, 2008). The observation that in those animals where the GluN2C subunit was downregulated do not show enhancement or a reduction in reward pursuit after the intracerebral injection of PPPA or Dhk, further support the idea that this particular NMDA receptor subtype is necessary for relying on the reward signal into DA cells. The reduction of this receptor activity decreased the overall responsivity of DA neurons to glutamate inputs. NMDA receptors containing the GluN2C subunit are characterized by low-conductance channel openings, a decrease in calcium permeability, reduced sensitivity to magnesium block, lack desensitization, and have a high affinity for Glutamate and glycine which may allow their activation by spillover glutamate (Cull-Candy, Brickley, & Farrant, 2001). These properties enable NMDA receptors containing the GluN2C subunit to be tonically active under resting conditions and confer them with a unique ability to influence neuronal excitability (Binshtok, Fleidervish, Sprengel, & Gutnick, 2006). The downregulations, in the expression of the GluN2C subunit, would indirectly hyperpolarize dopamine cells due to the increase in Ca^{2+} permeability entering the cell *via* NMDARs; which in turn activates small-conductance calcium-activated potassium (SK) channels promoting rapid membrane hyperpolarization and consequent magnesium (Mg^{2+}) block of the NMDARs (Creed et al., 2016; Ngo-Anh et al., 2005). This change in the activation threshold of DA neurons would make them unresponsive to changes in their inhibitory drive, and therefore unable to substantially change reward pursuit(see supplementary Fig.S3).

In conclusion, we demonstrated that a localized decrease on the GluN2C receptors of the VTA significantly alter the rewarding signal originated in the DR. This observation adds to other research suggesting that the GluN2C receptor play an important role in several disorders including drug abuse (Joffe & Grueter, 2016) and schizophrenia (Gupta et al., 2016; Hillman et al., 2011). Our results suggest that the levels of this receptor in the VTA might be at the root of anhedonia.

Acknowledgments The present research was supported by NSERC grant # 119057 to Pierre-Paul Rompré, Herbert H. Jasper fellowship to Giovanni Hernandez, CIHR operating grant #130407 to Daniel Lévesque.

Disclosure: The authors confirm that they don't have a conflict of interest related to these studies.

References

Allen Institute for Brain Science. (2010). Allen Mouse Brain Atlas. Retrieved from https://mouse.brain-map.org/search/index

Anderegg, A., Poulin, J. F., & Awatramani, R. (2015). Molecular heterogeneity of midbrain dopaminergic neurons - Moving toward single cell resolution. *FEBS Letters*, 589(24), 3714–3726. Retrieved from https://doi.org/10.1016/j.febslet.2015.10.022

Bergeron, S., & Rompré, P.-P. (2013). Blockade of ventral midbrain NMDA receptors enhances brain stimulation reward: a preferential role for GluN2A subunits. *European Neuropsychopharmacology : The Journal of the European College of Neuropsychopharmacology*, 23(11), 1623–35. Retrieved 28 April 2014 from https://doi.org/10.1016/j.euroneuro.2012.12.005

Binshtok, A. M., Fleidervish, I. A., Sprengel, R., & Gutnick, M. J. (2006). NMDA receptors in layer 4 spiny stellate cells of the mouse barrel cortex contain the NR2C subunit. *Journal of Neuroscience*, 26(2),

708–715. Retrieved from https://doi.org/10.1523/JNEUROSCI.4409-05.2006

Bonci, A., & Malenka, R. C. (1999). Properties and plasticity of excitatory synapses on dopaminergic and GABAergic cells in the ventral tegmental area. *The Journal of Neuroscience : The Official Journal of the Society for Neuroscience*, 19, 3723–3730.

Boye, S. M., & Rompré, P.-P. (1996). Mesencephalic substrate of reward: Axonal connections. *The Journal of Neuroscience*. US: Society for Neuroscience.

Carr, D. B., & Sesack, S. R. (2000). Projections from the rat prefrontal cortex to the ventral tegmental area: target specificity in the synaptic associations with mesoaccumbens and mesocortical neurons. *The Journal of Neuroscience : The Official Journal of the Society for Neuroscience*, 20(10), 3864–73. Retrieved from http://www.ncbi.nlm.nih.gov/pubmed/10804226

Chergui, K., Charléty, P. J., Akaoka, H., Saunier, C. F., Brunet, J. -L, Buda, M., … Chouvet, G. (1993a). Tonic Activation of NMDA Receptors Causes Spontaneous Burst Discharge of Rat Midbrain Dopamine Neurons In Vivo. *European Journal of Neuroscience*, 5(2), 137–144. Retrieved from https://doi.org/10.1111/j.1460-9568.1993.tb00479.x

Chergui, K., Charléty, P. J., Akaoka, H., Saunier, C. F., Brunet, J. L., Buda, M., … Chouvet, G. (1993b). Tonic activation of NMDA receptors causes spontaneous burst discharge of rat midbrain dopamine neurons in vivo. *The European Journal of Neuroscience*, 5(2), 137–44. Retrieved from http://www.ncbi.nlm.nih.gov/pubmed/8261095

Creed, M., Kaufling, J., Fois, G. R., Jalabert, M., Yuan, T., Lüscher, C., … Bellone, C. (2016). Cocaine exposure enhances the activity of ventral tegmental area dopamine neurons via calcium-impermeable NMDARs. *Journal of Neuroscience*, 36(42), 10759–10768. Retrieved from https://doi.org/10.1523/JNEUROSCI.1703-16.2016

Cull-Candy, S., Brickley, S., & Farrant, M. (2001). NMDA receptor subunits: diversity, development and disease. *Current Opinion in Neurobiology*, 11(3), 327–35. Retrieved from https://doi.org/10.1016/s0959-4388(00)00215-4

Ducrot, C., Fortier, E., Bouchard, C., & Rompré, P.-P. (2013). Opposite modulation of brain stimulation reward by NMDA and AMPA receptors in the ventral tegmental area. *Frontiers in Systems Neuroscience*, 7(October), 57. Retrieved 28 April 2014 from https://doi.org/10.3389/fnsys.2013.00057

Grace, A. A., & Bunney, B. S. (1984). The control of firing pattern in nigral dopamine neurons: burst firing. *The Journal of Neuroscience : The Official Journal of the Society for Neuroscience*, 4, 2877–2890. Retrieved from https://doi.org/6150071

Gupta, S. C., Ravikrishnan, A., Liu, J., Mao, Z., Pavuluri, R., Hillman, B. G., … Dravid, S. M. (2016). The NMDA receptor GluN2C subunit controls cortical excitatory-inhibitory balance, neuronal oscillations and cognitive function. *Scientific Reports*, 6(December), 1–13. Retrieved from https://doi.org/10.1038/srep38321

Hernandez, G., Trujillo-Pisanty, I., Cossette, M.-P., Conover, K., & Shizgal, P. (2012). Role of Dopamine Tone in the Pursuit of Brain Stimulation Reward. *Journal of Neuroscience*, 32(32), 11032–11041. Retrieved 25 October 2012 from https://doi.org/10.1523/JNEUROSCI.1051-12.2012

Hernandez, Giovanni, Breton, Y.-A., Conover, K., & Shizgal, P. (2010). At what stage of neural processing does cocaine act to boost pursuit of rewards? *PloS One*, 5(11), e15081. Retrieved 21 November 2012 from https://doi.org/10.1371/journal.pone.0015081

Hernandez, Giovanni, Cossette, M. P., Shizgal, P., & Rompré, P. P. (2016). Ventral midbrain NMDA receptor blockade: From enhanced reward and dopamine inactivation. *Frontiers in Behavioral*

Neuroscience, 10(August), 1–11. Retrieved from https://doi.org/10.3389/fnbeh.2016.00161

Hernandez, Giovanni, Khodami-Pour, A., Lévesque, D., & Rompré, P.-P. P. (2015). Reduction in Ventral Midbrain NMDA Receptors Reveals Two Opposite Modulatory Roles for Glutamate on Reward. *Neuropsychopharmacology*, 40(7), 1682–1691. Retrieved from https://doi.org/10.1038/npp.2015.14

Hillman, B. G., Gupta, S. C., Stairs, D. J., Buonanno, A., & Dravid, S. M. (2011). Behavioral analysis of NR2C knockout mouse reveals deficit in acquisition of conditioned fear and working memory. *Neurobiology of Learning and Memory*, 95(4), 404–414. Retrieved from https://doi.org/10.1016/j.nlm.2011.01.008

Hyland, B. I., Reynolds, J. N. J., Hay, J., Perk, C. G., & Miller, R. (2002). Firing modes of midbrain dopamine cells in the freely moving rat. *Neuroscience*, 114(2), 475–492. Retrieved from https://doi.org/10.1016/S0306-4522(02)00267-1

Jacobs, B. L., & Azmitia, E. C. (1992). Structure and function of the brain serotonin system. *Physiological Reviews*, 72(1), 165–230. Retrieved from https://doi.org/10.1152/physrev.1992.72.1.165

Joffe, M. E., & Grueter, B. A. (2016). Cocaine Experience Enhances Thalamo-Accumbens N-Methyl-D-Aspartate Receptor Function. *Biological Psychiatry*, 80(9), 671–681. Retrieved from https://doi.org/10.1016/j.biopsych.2016.04.002

Johnson, S. W., Seutin, V., & North, R. A. (1992). Burst firing in dopamine neurons induced by N-methyl-D-aspartate: Role of electrogenic sodium pump. *Science*, 258(5082), 665–667. Retrieved from https://doi.org/10.1126/science.1329209

Lein, E. S., Hawrylycz, M. J., Ao, N., Ayres, M., Bensinger, A., Bernard, A., … Jones, A. R. (2007). Genome-wide atlas of gene expression in the adult mouse brain. *Nature*, 445(7124), 168–176. Retrieved

from https://doi.org/10.1038/nature05453

Liu, Z., Zhou, J., Li, Y., Hu, F., Lu, Y., Ma, M., … Luo, M. (2014). Dorsal Raphe Neurons Signal Reward through 5-HT and Glutamate. *Neuron*, 81(6), 1360–74. Retrieved 28 April 2014 from https://doi.org/10.1016/j.neuron.2014.02.010

Mcdevitt, R. A., Tiran-cappello, A., Harvey, B. K., Bonci, A., Shen, H., Balderas, I., … Marino, R. A. M. (2014). Serotonergic versus Nonserotonergic Dorsal Raphe Projection Neurons : Differential Participation in Reward Article Serotonergic versus Nonserotonergic Dorsal Raphe Projection Neurons : Differential Participation in Reward Circuitry, 1857–1869.

McIlhinney, R. A. J., Le Bourdellès, B., Molnár, E., Tricaud, N., Streit, P., & Whiting, P. J. (1998). Assembly intracellular targeting and cell surface expression of the human N-methyl-D-aspartate receptor subunits NR1a and NR2A in transfected cells. *Neuropharmacology*, 37(10–11), 1355–1367. Retrieved from https://doi.org/10.1016/S0028-3908(98)00121-X

Miliaressis, E., Rompre, P. P., Laviolette, P., Philippe, L., & Coulombe, D. (1986). The curve-shift paradigm in self-stimulation. *Physiology & Behavior*, 37, 85–91. Retrieved from https://doi.org/10.1016/0031-9384(86)90388-4

Moisan, J., & Rompre, P. P. (1998). Electrophysiological evidence that a subset of midbrain dopamine neurons integrate the reward signal induced by electrical stimulation of the posterior mesencephalon. *Brain Research*, 786(1), 143–152. Retrieved from https://doi.org/doi:10.1016/S0006-8993(97)01457-1

Monyer, H., Burnashev, N., Laurie, D. J., Sakmann, B., & Seeburg, P. H. (1994). Developmental and regional expression in the rat brain and functional properties of four NMDA receptors. *Neuron*, 12(3), 529–540. Retrieved from https://doi.org/10.1016/0896-6273(94)90210-0

Monyer, H., Sprengel, R., Schoepfer, R., Herb, A., Higuchi, M., Lomeli, H., … Seeburg, P. H. (1992). Heteromeric NMDA Receptors: Molecular and Functional Distinction of Subtypes. *Science*, 256(5060), 1217–1221. Retrieved from https://doi.org/10.1126/science.256.5060.1217

Nakanishi, S. (1992). Molecular diversity of glutamate receptors and implications for brain function. *Science*, 258(5082), 597–603. Retrieved from https://doi.org/10.1126/science.1329206

Ngo-Anh, T. J., Bloodgood, B. L., Lin, M., Sabatini, B. L., Maylie, J., & Adelman, J. P. (2005). SK channels and NMDA receptors form a Ca2+-mediated feedback loop in dendritic spines. *Nature Neuroscience*, 8(5), 642–649. Retrieved from https://doi.org/10.1038/nn1449

Nugent, F. S., & Kauer, J. A. (2008). LTP of GABAergic synapses in the ventral tegmental area and beyond. *The Journal of Physiology*, 586(6), 1487–93. Retrieved 21 August 2014 from https://doi.org/10.1113/jphysiol.2007.148098

Omelchenko, N., & Sesack, S. R. (2009). Ultrastructural analysis of local collaterals of rat ventral tegmental area neurons: GABA phenotype and synapses onto dopamine and GABA cells. *Synapse (New York, N.Y.)*, 63(10), 895–906. Retrieved 30 April 2014 from https://doi.org/10.1002/syn.20668

Overton, P., & Clark, D. (1992). Iontophoretically administered drugs acting at the N-methyl-D-aspartate receptor modulate burst firing in A9 dopamine neurons in the rat. *Synapse (New York, N.Y.)*, 10, 131–140. Retrieved from https://doi.org/10.1002/syn.890100208

Overton, P. G., & Clark, D. (1997). Burst firing in midbrain dopaminergic neurons. *Brain Research. Brain Research Reviews*, 25(3), 312–34. Retrieved from http://www.ncbi.nlm.nih.gov/pubmed/9495561

Parker, J. G., Zweifel, L. S., Clark, J. J., Evans, S. B., Phillips, P. E. M., & Palmiter, R. D. (2010). Absence of NMDA receptors in dopamine neurons attenuates dopamine release but not conditioned approach

during Pavlovian conditioning. *Proceedings of the National Academy of Sciences of the United States of America*, 107(30), 13491–13496. Retrieved from https://doi.org/10.1073/pnas.1007827107

Pérez-Otaño, I., Schulteis, C. T., Contractor, A., Lipton, S. A., Trimmer, J. S., Sucher, N. J., & Heinemann, S. F. (2001). Assembly with the NR1 subunit is required for surface expression of NR3A-containing NMDA receptors. *Journal of Neuroscience*, 21(4), 1228–1237. Retrieved from https://doi.org/10.1523/jneurosci.21-04-01228.2001

Poulin, J. F., Gaertner, Z., Moreno-Ramos, O. A., & Awatramani, R. (2020). Classification of Midbrain Dopamine Neurons Using Single-Cell Gene Expression Profiling Approaches. *Trends in Neurosciences*, 43(3), 155–169. Retrieved from https://doi.org/10.1016/j.tins.2020.01.004

Qi, J., Zhang, S., Wang, H.-L., Wang, H., de Jesus Aceves Buendia, J., Hoffman, A. F., … Morales, M. (2014). A glutamatergic reward input from the dorsal raphe to ventral tegmental area dopamine neurons. *Nature Communications*, 5(May), 5390. Retrieved 12 November 2014 from https://doi.org/10.1038/ncomms6390

Ravikrishnan, A., Gandhi, P. J., Shelkar, G. P., Liu, J., Pavuluri, R., & Dravid, S. M. (2018). Region-specific Expression of NMDA Receptor GluN2C Subunit in Parvalbumin-Positive Neurons and Astrocytes: Analysis of GluN2C Expression using a Novel Reporter Model. *Neuroscience*, 380, 49–62. Retrieved from https://doi.org/10.1016/j.neuroscience.2018.03.011

Rompre, P. P., & Miliaressis, E. (1985). Pontine and mesencephalic substrates of self-stimulation. *Brain Research*, 359(1–2), 246–59. Retrieved from http://www.ncbi.nlm.nih.gov/pubmed/4075148

Rompré, P. P., & Miliaressis, E. (1987). Behavioral determination of refractory periods of the brainstem substrates of self-stimulation. *Behavioural Brain Research*, 23(3), 205–19. Retrieved from

http://www.ncbi.nlm.nih.gov/pubmed/3580107

Salahpour, A., Medvedev, I. O., Beaulieu, J.-M., Gainetdinov, R. R., & Caron, M. G. (2007). Local knockdown of genes in the brain using small interfering RNA: a phenotypic comparison with knockout animals. *Biological Psychiatry*, 61(1), 65–9. Retrieved 16 May 2014 from https://doi.org/10.1016/j.biopsych.2006.03.020

Salamone, J. D. (1991). Behavioral pharmacology of dopamine systems: A new synthesis. In *The mesolimbic dopamine system: From motivation to action* (pp. 599–614).

Saunders, A., Macosko, E. Z., Wysoker, A., Goldman, M., Krienen, F. M., de Rivera, H., … McCarroll, S. A. (2018). Molecular Diversity and Specializations among the Cells of the Adult Mouse Brain. *Cell*, 174(4), 1015-1030.e16. Retrieved from https://doi.org/10.1016/j.cell.2018.07.028

Schultz, W. (1997). A Neural Substrate of Prediction and Reward. *Science*, 275(5306), 1593–1599. Retrieved 6 February 2013 from https://doi.org/10.1126/science.275.5306.1593

Sesack, S. R., Carr, D. B., Omelchenko, N., & Pinto, A. (2003). Anatomical Substrates for Glutamate-Dopamine Interactions. *Annals of the New York Academy of Sciences*, 1003(1), 36–52. Retrieved from https://doi.org/10.1196/annals.1300.066

Shelkar, G. P., Pavuluri, R., Gandhi, P. J., Ravikrishnan, A., Gawande, D. Y., Liu, J., … Dravid, S. M. (2019). Differential effect of NMDA receptor GluN2C and GluN2D subunit ablation on behavior and channel blocker-induced schizophrenia phenotypes. *Scientific Reports*, 9(1), 1–11. Retrieved from https://doi.org/10.1038/s41598-019-43957-2

Simon, H., Le Moal, M., & Cardo, B. (1976). Intracranial self-stimulation from the dorsal raphe nucleus of the rat: effects of the injection of para-chlorophenylalanine and of alpha-methylparatyrosine. *Behavioral Biology*. Retrieved from https://doi.org/10.1016/S0091-6773(76)91486-3

Stellar, J. R., Kelley, a E., & Corbett, D. (1983). Effects of peripheral and central dopamine blockade on lateral hypothalamic self-stimulation: evidence for both reward and motor deficits. *Pharmacology, Biochemistry, and Behavior*, 18(3), 433–42. Retrieved from http://www.ncbi.nlm.nih.gov/pubmed/6835998

Suaud-Chagny, M. F., Chergui, K., Chouvet, G., & Gonon, F. (1992). Relationship between dopamine release in the rat nucleus accumbens and the discharge activity of dopaminergic neurons during local in vivo application of amino acids in the ventral tegmental area. *Neuroscience*. Retrieved from https://doi.org/10.1016/0306-4522(92)90076-E

Tsai, H.-C., Zhang, F., Adamantidis, A., Stuber, G. D., Bonci, A., de Lecea, L., & Deisseroth, K. (2009). Phasic firing in dopaminergic neurons is sufficient for behavioral conditioning. *Science (New York, N.Y.)*, 324(5930), 1080–4. Retrieved 10 July 2014 from https://doi.org/10.1126/science.1168878

Vasudeva, R. K., Lin, R. C. S., Simpson, K. L., & Waterhouse, B. D. (2011). Functional organization of the dorsal raphe efferent system with special consideration of nitrergic cell groups. *Journal of Chemical Neuroanatomy*, 41(4), 281–293. Retrieved from https://doi.org/10.1016/j.jchemneu.2011.05.008

Wang, R. Y., & Aghajani, G. K. (1977). Antidromically identified serotonergic neurons in the rat midbrain raphe: evidence for collateral inhibition. *Brain Research*. Retrieved from https://doi.org/10.1016/0006-8993(77)90719-3

Watabe-Uchida, M., Zhu, L., Ogawa, S. K., Vamanrao, A., & Uchida, N. (2012). Whole-brain mapping of direct inputs to midbrain dopamine neurons. *Neuron*, 74(5), 858–73. Retrieved 28 April 2014 from https://doi.org/10.1016/j.neuron.2012.03.017

Wenzel, A., Scheurer, L., Künzi, R., Fritschy, J. M., Mohler, H., & Benke, D. (1995). Distribution of NMDA receptor subunit proteins NR2A, 2B, 2C and 2D in rat brain. *Neuroreport*, 7(1), 45–8. Retrieved

from http://www.ncbi.nlm.nih.gov/pubmed/8742413

Wise, R a, & Rompre, P. P. (1989). Brain dopamine and reward. *Annual Review of Psychology*, 40, 191–225. Retrieved from https://doi.org/10.1146/annurev.ps.40.020189.001203

Wise, Roy a. (2004). Dopamine, learning and motivation. *Nature Reviews. Neuroscience*, 5(6), 483–94. Retrieved 9 July 2014 from https://doi.org/10.1038/nrn1406

You, Z. B., Chen, Y. Q., & Wise, R. A. (2001). Dopamine and glutamate release in the nucleus accumbens and ventral tegmental area of rat following lateral hypothalamic self-stimulation. *Neuroscience*, 107, 629–639. Retrieved from https://doi.org/10.1016/S0306-4522(01)00379-7

Zweifel, L. S., Parker, J. G., Lobb, C. J., Rainwater, A., Wall, V. Z., Fadok, J. P., … Palmiter, R. D. (2009). Disruption of NMDAR-dependent burst firing by dopamine neurons provides selective assessment of phasic dopamine-dependent behavior. *Proceedings of the National Academy of Sciences*, 106(18), 7281–7288. Retrieved from https://doi.org/10.1073/pnas.0813415106

Figure Captions

Figure 1. Relative expression of NMDAR Grin2 subunits mRNA across different brain areas. Brain punches from the prefrontal cortex (PFC), nucleus accumbens (Nac), lateral hypothalamus (LH), habenula (Hab), amygdala (Amyg), bed nucleus of the stria terminalis (BNST), ventral pallidum (VP), hippocampus (Hipp), pedunculopontine tegmental nucleus (PPtg), ventral tegmental area (VTA), rostromedial tegmental nucleus (RMtg) and raphe nucleus (Raphe were analyzed) (n=4). Relative mRNA levels were quantified using $\Delta\Delta$ ct method. Histogram bars represent relative mRNA levels normalized over both Gapdh and Hprt mRNA levels.

Figure 2. Double FISH immunodetection shows a high colocalization of Grin2c in TH positive cells of the VTA. A. Representative images of the ventral midbrain area containing the SN and VTA taken from the Allen Brain Atlas, displaying Grin2c transcript in the red nucleus (arrowhead) and SN and VTA area (arrow). B-B". Fluorescent *in situ* hybridization reveals that Grin2c expression (Fluorescein; green) overlaps with Th (Cy3; red) in the mesencephalon, scale represents 50 µm. **C.** Bar graphs showing the count of Th and Grin2c positive cells in the VTA.

Figure 3. Grin2c intra-VTA siRNA injections significantly reduce GluN2C protein levels in the VTA. A) siRNA microinjections against NMDAR Grin2c subunit produces a significant reduction in this subunit immunoreactivity. The histogram bars represent means +/- SEM of normalized NMDAR GluN2C subunit protein levels in animals injected with the Grin2c siRNA or the negative control siRNA (N=12 per condition) (*p <0.05; Student's t-test) in VTA homogenates. The inset shows representative examples of signals from GluN2C and β-actin after Western blotting procedure. **B)** The histogram bars represent means +/- SEM of normalized NMDAR GluN2A subunit protein levels in animals injected with the Grin2c siRNA or the negative control siRNA (N=12 per condition) in VTA homogenates. The inset shows representative examples of signals from GluN2A and β-actin after Western blotting procedure.

Figure 4. Intra-VTA Grin2c siRNA injection reduced rate-frequency response from dorsal raphe stimulation. The figure shows representative rate-frequency curves for selected subjects showing the effect of the different siRNA treatment and intra-VTA injection of PPPA (0.825 nmol/0.5µl/side) or Dhk (5 nmol/0.5µl/side). **A-A')** Treatment with the negative control siRNA (0.5 µg/side) produced no effect on the curve that relates the nose-poke rate with the electrical pulse trains. The baseline curve and the one obtained 24-h after the first and second siRNA injections overlap. **B)** In the animals treated with the negative control siRNA Intra-VTA injection with PPPA produced a leftward and upward shift of rate-frequency curve; whereas, **B')** intra-VTA injection with Dhk produced a rightward and downward shift of rate-frequency curve. **C-C')** Treatment with siRNA (0.5µg /side) against Grin2c produced a decrease of the rewarding effects that arise from the dorsal raphe electrical stimulation. The dark-red curve obtained 24-h after the last siRNA injection is displaced to the right, and there is a decrease in the upper asymptote when contrasted against the baseline curves that are shown in blue. Interestingly, the Grin2c siRNA treatment alters PPPA effect. **D, D')** siRNA injections against Grin2c obliterate the effects of PPPA and Dhk on reward-seeking and motor performance. The pretreatment with the Grin2c siRNA renders these drugs ineffective for modifying the reward signal that arises from dorsal raphe stimulation.

Figure 5. Shifts caused by control and Grin2c siRNAs in stimulation threshold and maximum response rate. A) Histogram bars represent means +/- SEM of M50 in animals that received control of Grin2c siRNA after raphe stimulation. Treatment with the control siRNA did not produce a significant change in the stimulation threshold (M50), but the treatment with the siRNA against the Grin2c subunit produces a significant increase (*p <0.05; Student's t test). **B)** The siRNA against Grin2c produced a significant decrease in the maximum response rate (*p <0.05; Student's t test) compared to subjects that received the scramble siRNA. The gray area denotes the 95% confidence interval of the baseline curves.

Figure 6. Shifts caused by intra-VTA injections of PPPA or Dhk in stimulation threshold and maximum response rate. A) siRNA downregulation of the Grin2c subunit in the VTA abolishes the enhancing effect of PPPA. PPPA produced a decrease in the self-stimulation threshold only in those animals that were pre-treated with the scrambled siRNA. The self-stimulation threshold showed no reliable change in those animals pre-treated with the siRNA against Grin2c. The PPPA enhancement effect on M50 values in the scrambled siRNA group is significantly different from that of the group that received the siRNA against Grin2c **B)** Similarly, PPPA only produced an increase in the maximum response rate in those animals that were pre-treated with the scrambled siRNA and not with the siRNA against Grin2c **C)** siRNA downregulation of Grin2c in the VTA abolishes the attenuation effect of Dhk on reward. Dhk only produced an increase in the M50 values on those animals that received the scramble siRNA **D)**Dhk only produced a decrease in the maximum response rate in the animals pre-treated with the scramble siRNA. The gray area denotes the 95% confidence interval of the baseline curves. (*p <0.05; Student's t-test).

Supplementary Figure 1: Schematic of the experimental behavioral procedure.

Supplementary Figure 2: Low-level magnification of Double FISH immunodetection.

Supplementary Figure 3: A proposed working model of the activation of GluN2C in reward pursuit. A) Glutamate neurotransmission coming from DR afferents activate DA neurons by binding into GluN2C receptors and facilitating phasic burst firing. **B)** Downregulation of GuN2C produces an increase in Ca^{2+} permeability and hyperpolarization of DA neurons, increasing their activation threshold.

Supplemetary Table 1: Primer sequences for qPCR Grin2 analysis

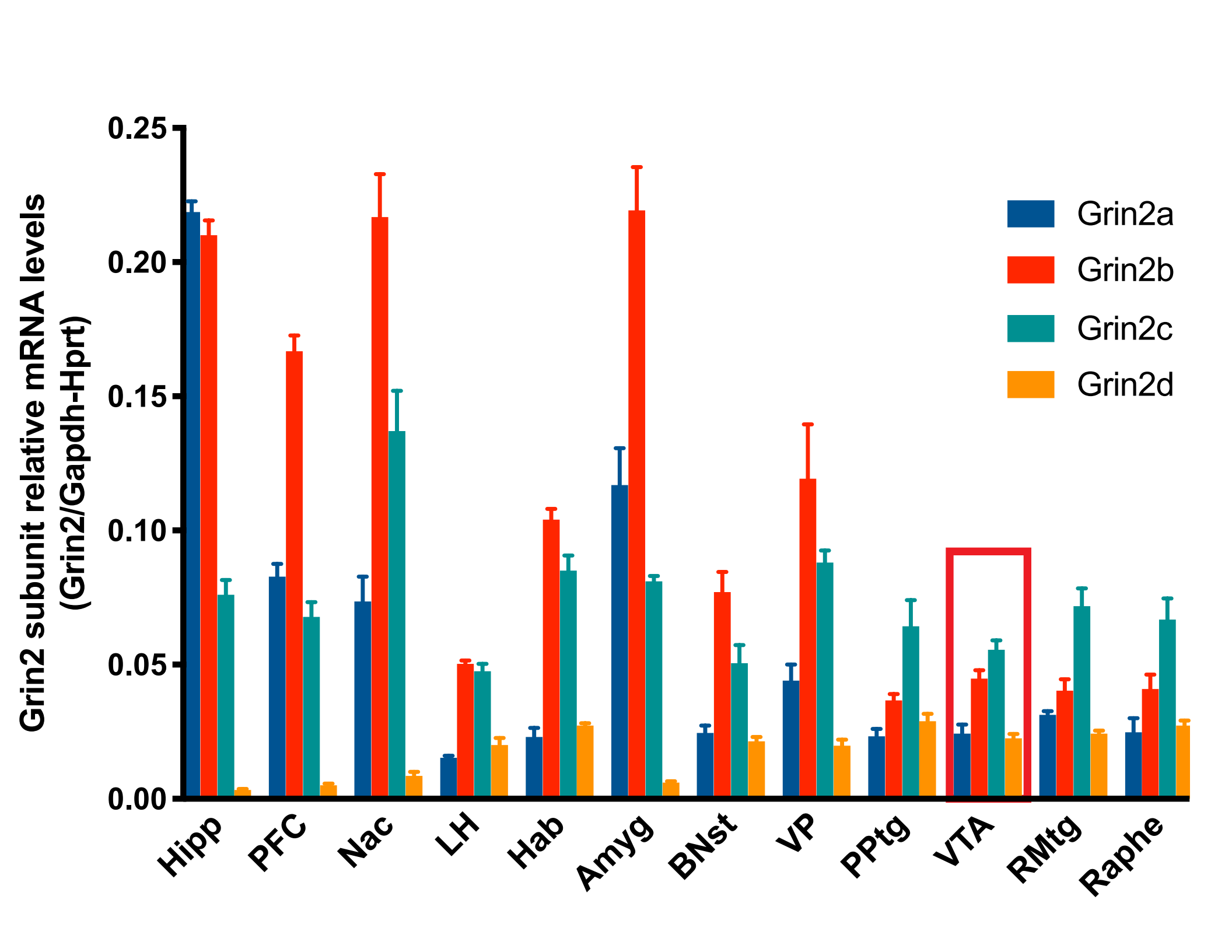
Grin2 subunit relative mRNA levels
(Grin2/Gapdh-Hprt)
0.25
0.20
0.15
0.10
0.05
0.00
Grin2a
Grin2b
Grin2c
Grin2d
Hipp
PFC
Nac
LH
Hab
Amyg
BNst
VP
PPtg
VTA
RMtg
Raphe

A

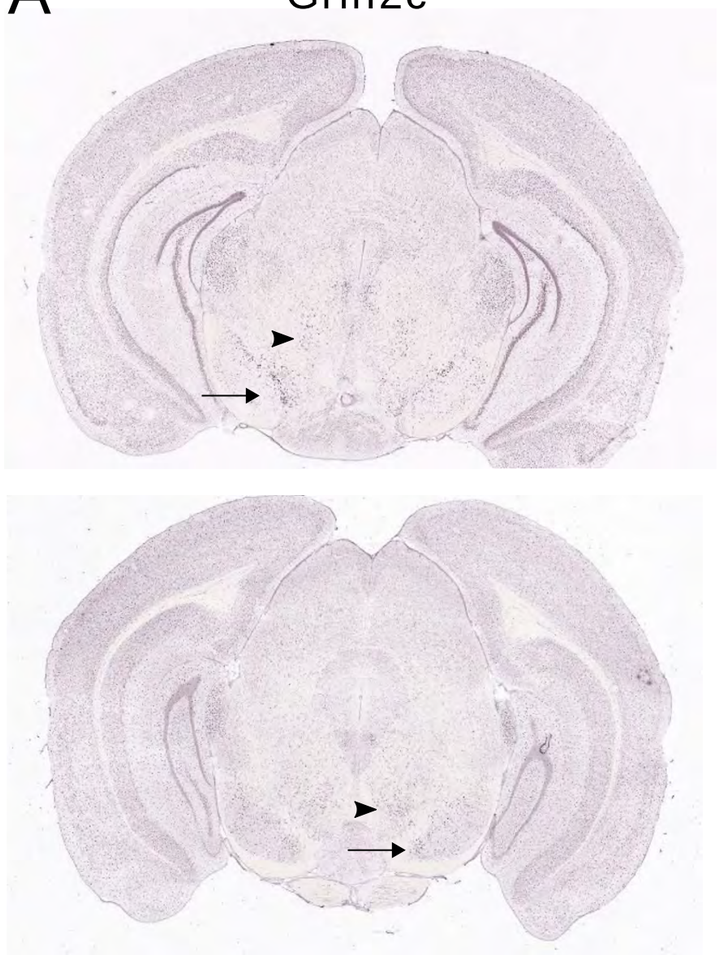

Allen Brain Atlas

B

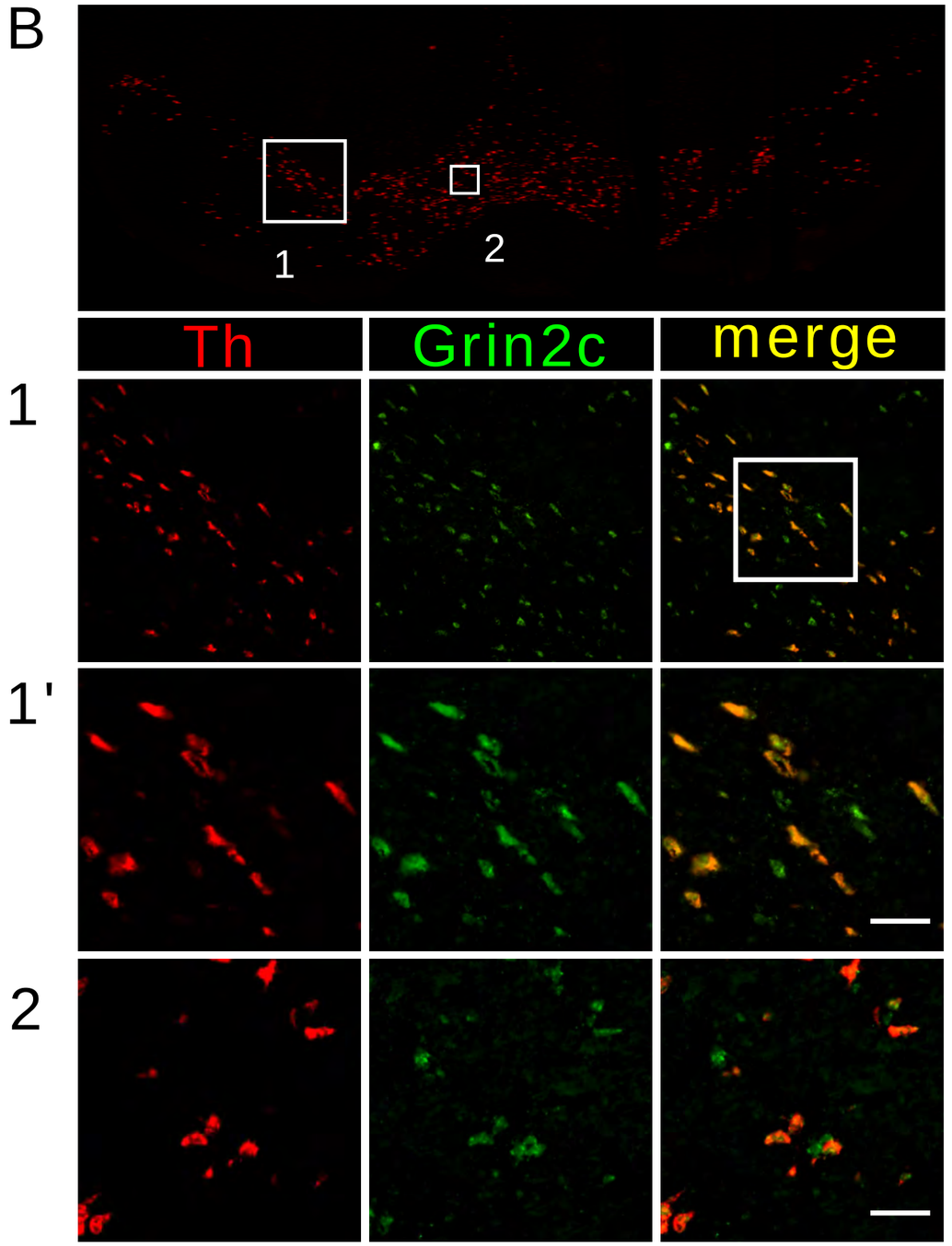

C

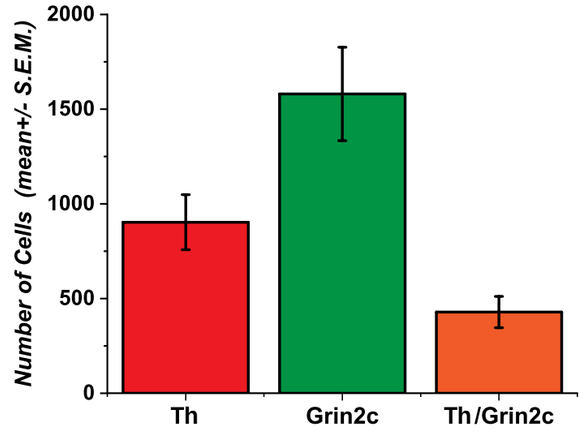

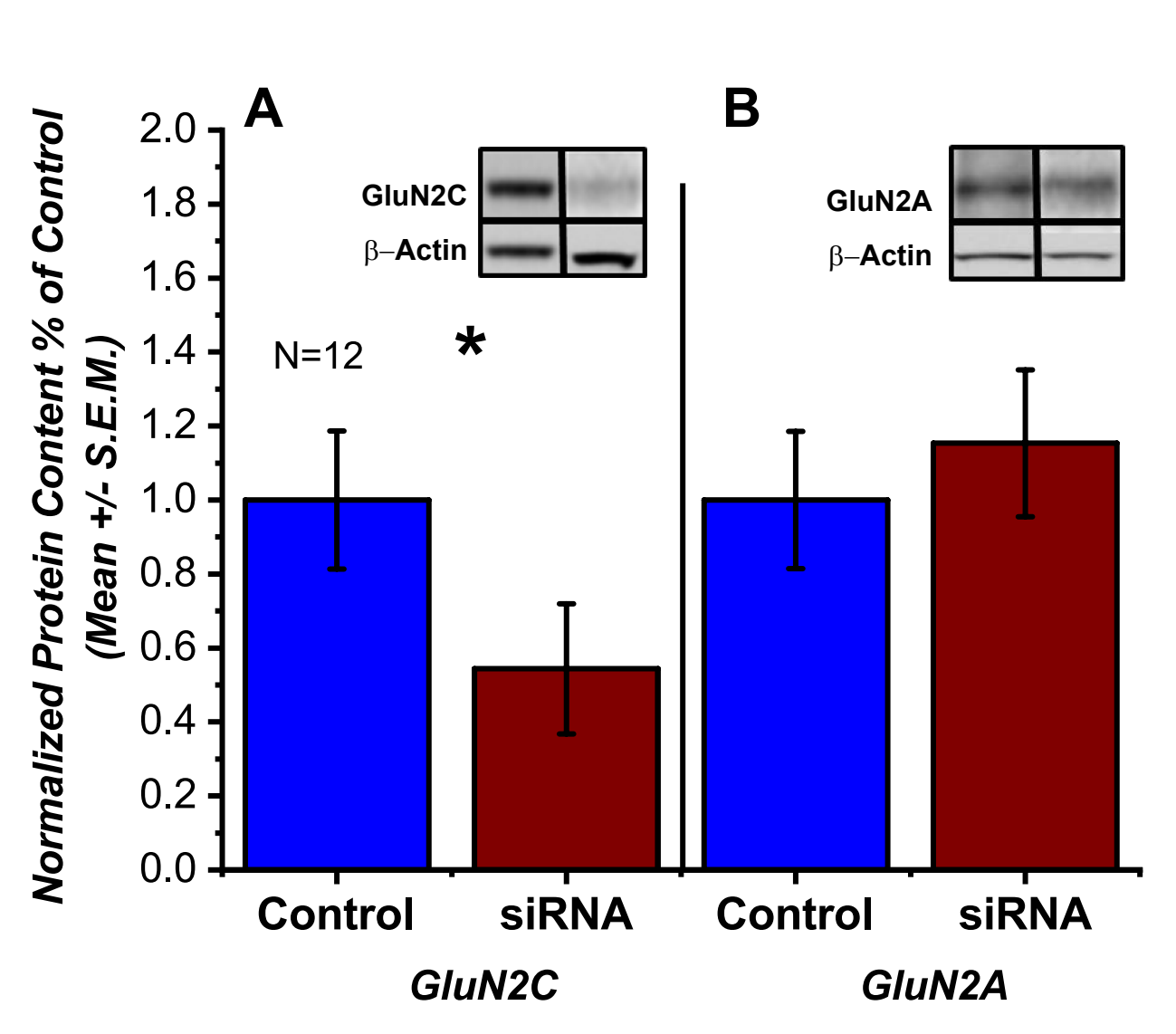
A
B
GluN2C
β–Actin
GluN2A
β–Actin
N=12
*
Normalized Protein Content % of Control
(Mean +/- S.E.M.)
2.0
1.8
1.6
1.4
1.2
1.0
0.8
0.6
0.4
0.2
0.0
Control
siRNA
Control
siRNA
GluN2C
GluN2A

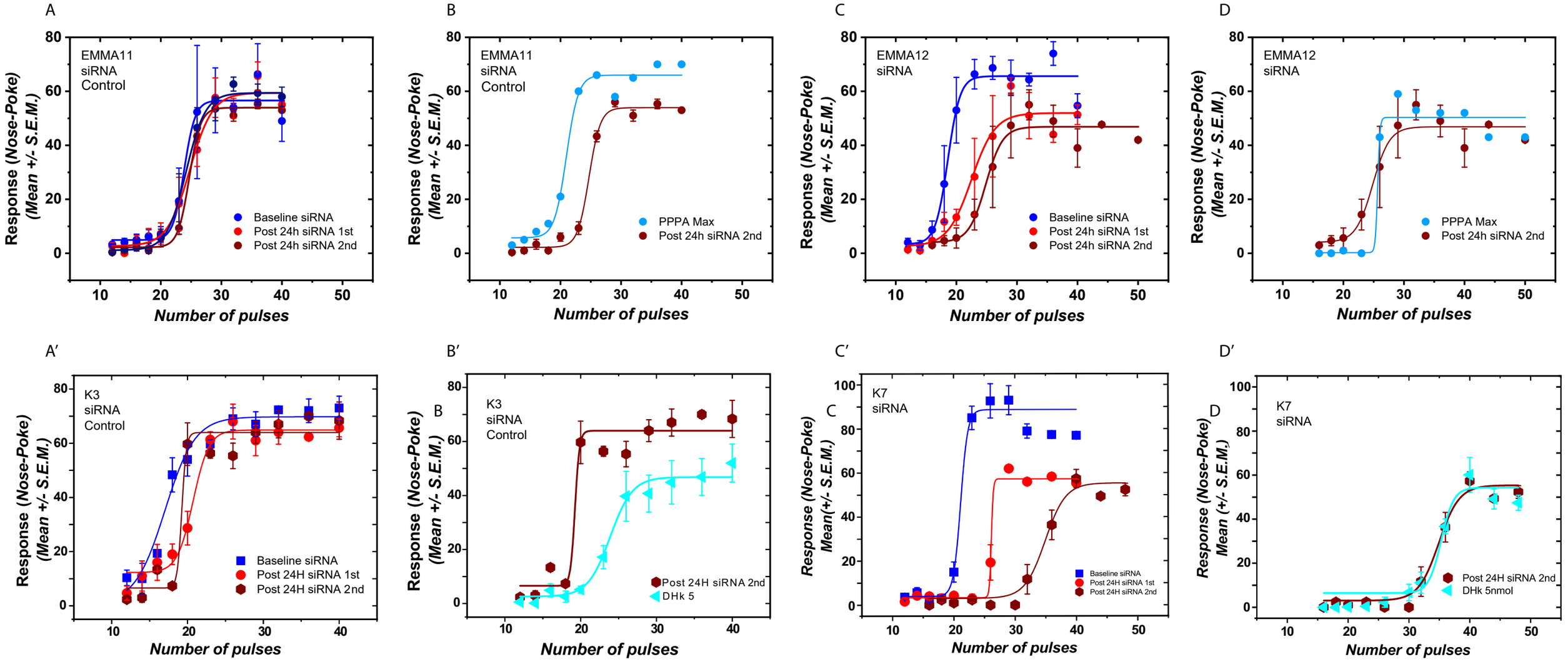
A
EMMA11
siRNA
Control
Baseline siRNA
Post 24h siRNA 1st
Post 24h siRNA 2nd
Response (Nose-Poke)
(Mean +/- S.E.M.)
Number of pulses
B
EMMA11
siRNA
Control
PPPA Max
Post 24h siRNA 2nd
C
EMMA12
siRNA
Baseline siRNA
Post 24h siRNA 1st
Post 24h siRNA 2nd
D
EMMA12
siRNA
PPPA Max
Post 24h siRNA 2nd
A′
K3
siRNA
Control
Baseline siRNA
Post 24H siRNA 1st
Post 24H siRNA 2nd
B′
K3
siRNA
Control
Post 24H siRNA 2nd
DHk 5
C′
K7
siRNA
Baseline siRNA
Post 24H siRNA 1st
Post 24H siRNA 2nd
Response (Nose-Poke)
Mean(+/- S.E.M.)
D′
K7
siRNA
Post 24H siRNA 2nd
DHk 5nmol
Response (Nose-Poke)
Mean (+/- S.E.M.)

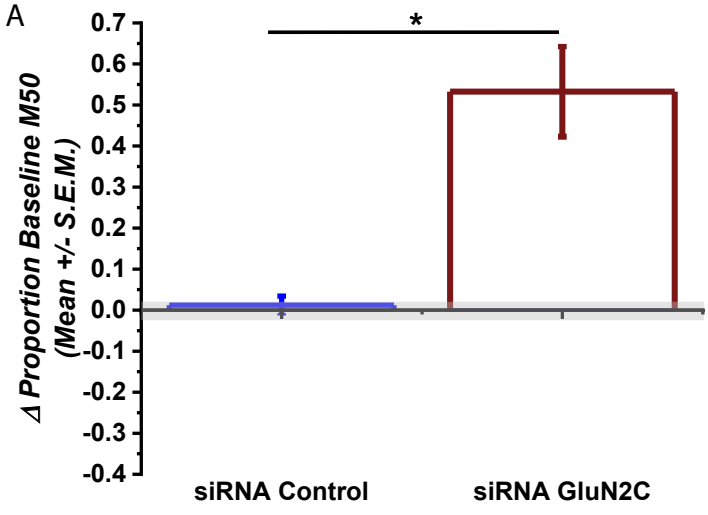
A
Δ Proportion Baseline M50
(Mean +/- S.E.M.)
0.7
0.6
0.5
0.4
0.3
0.2
0.1
0.0
-0.1
-0.2
-0.3
-0.4
*
siRNA Control
siRNA GluN2C

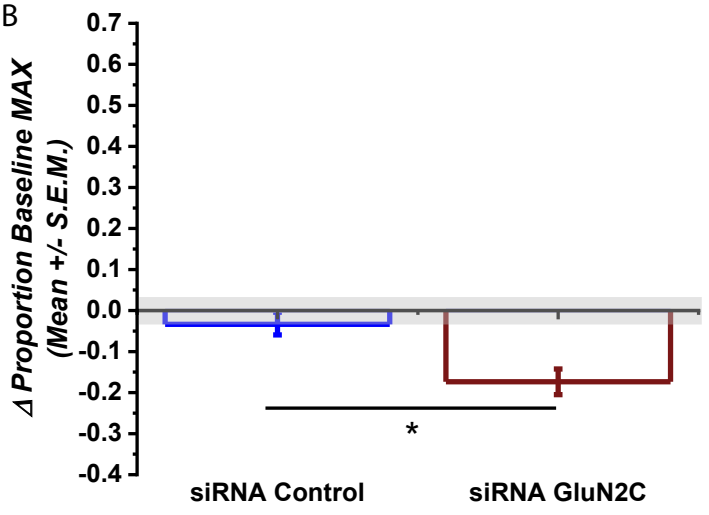
B
Δ Proportion Baseline MAX
(Mean +/- S.E.M.)
0.7
0.6
0.5
0.4
0.3
0.2
0.1
0.0
-0.1
-0.2
-0.3
-0.4
*
siRNA Control
siRNA GluN2C

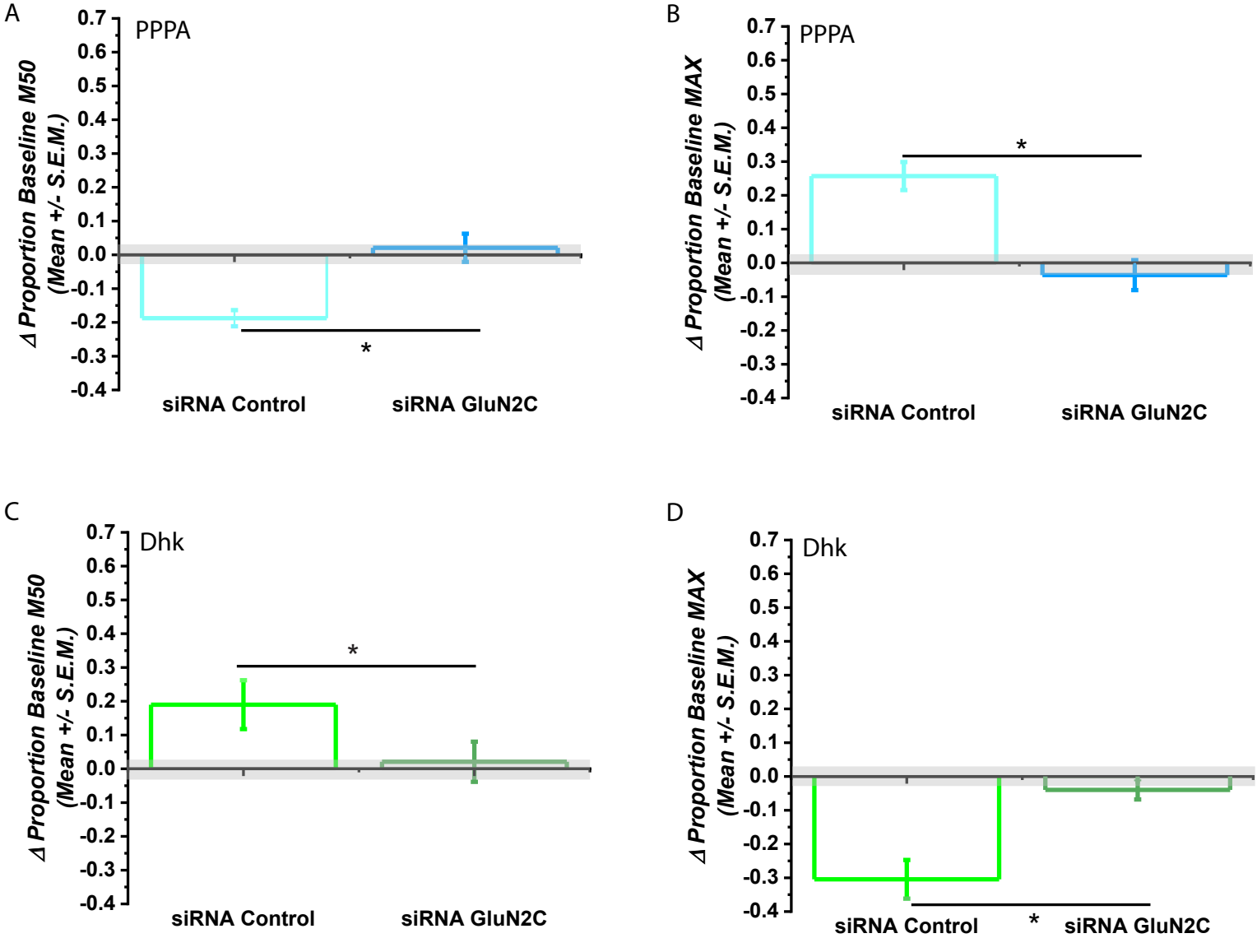
A
PPPA
Δ Proportion Baseline M50
(Mean +/- S.E.M.)
0.7
0.6
0.5
0.4
0.3
0.2
0.1
0.0
-0.1
-0.2
-0.3
-0.4
*
siRNA Control
siRNA GluN2C
B
PPPA
Δ Proportion Baseline MAX
(Mean +/- S.E.M.)
*
siRNA Control
siRNA GluN2C
C
Dhk
Δ Proportion Baseline M50
(Mean +/- S.E.M.)
*
siRNA Control
siRNA GluN2C
D
Dhk
Δ Proportion Baseline MAX
(Mean +/- S.E.M.)
siRNA Control
*
siRNA GluN2C